

has a trend which suggests the small circle does not perfectly fit the topographic data and the center should be moved slightly toward the east. The quantification of these and other morphological parameters evident in the new projection may yield insights into the kinematics of arc-normal slip and the partition of along-arc slip, and perhaps details of the rupture zones of great earthquakes.

G42D-4 1605h INVITED

**Raikot Fault and the Unusual Exhumation of the Nanga Parbat-Haramosh Massif, North Pakistan**

Mohammad Riaz ; D.J.Anastasio; P.K.Zeitler; A.S.Meltzer (EES, Lehigh University, 31 Williams Drive, Bethlehem, Pa-18015; ph. 610-758-5393; e-mail: mnr5@lehigh.edu); W.S.F.Kidd; M.A.Edwards (DEAS, SUNY at Albany, NY-12222; L.Seeber (LD-GEO, Palisades, NY-10964;

The Nanga Parbat Haramosh Massif (NPHM) is the northern most window of the Indian crust (basement gneisses and metasediments) exposed beneath Kohistan-Ladakh series (KLS) (island arcrocks) in Pakistan. The Main Mantle Thrust (MMT) is the midcrustal exposure of the Eocene suture and juxtaposes the Indian crust with the KLS. The MMT, on the western margin of the NPHM, is truncated by Raikot fault, which is characterized by NS to NESW strike and 45°80° E dip, crosscutting the foliation, brittle deformation, occasional cataclastites (1.1m, unfoliated, cm fragments), extensive occurrence of hot springs, large steps in river gradients and extreme topographic relief (5000 m) across the fault. Stratigraphic offsets and shear fibers suggest reverse motion on the fault. Similarly, northwestward tilting and overturned folding of fluviofacial sediments in the footwall of the fault (at Indus and Bunar valleys) is also consistent with reverse motion on the fault. Kinematic analysis of minor fault suites from within the Raikot fault zone indicate principal shortening orthogonal to the fault along the northern and southern portions and oblique in the central portion. The strain inversion in the middle part seems to be associated with the change in the strike of the fault. Absence of feldspar ductile deformation and presence of shear fibers, pressure solution in quartz along mesoscopic fault surfaces in the Raikot fault zone indicate deformation at greenschist facies conditions. Shallow level origin of the fault is obvious from the cataclastites presence and absence of ductile fabric. Maximum stratigraphic separation and high strain in middle part (basement gneisses over alluvium) and minimum separation and lesser strain on either end of the fault (metasediments over Kohistan) has not only resulted in local anatexis of the hanging-wall rocks but might also explain the unusual exhumation of the massif in its central part.

G42D-5 1620h INVITED

**Geochronological constraints on the geometry and timing of anatexis and exhumation at Nanga Parbat: A progress report.**

D A Schneider, P K Zeitler (both at: Earth and Environ Sci, Lehigh University, Bethlehem, PA 18015; dasd@lehigh.edu); M A Edwards, W S F Kidd (both at: Dept of Geological Sci, State University of New York at Albany, Albany, NY 12222)

We report single-grain, single-spot ion microprobe analyses of zircons and monazites from basement rocks and granites of the Nanga Parbat-

Haramosh Massif (NPHM) which substantially extend the constraints available on anatexis in the region. Two dikes from the Rupal Valley, south of Nanga Parbat summit yield, respectively, a monazite age of ~1.2 Ma and monazite and zircon ages of ~2.2 Ma. Similarly, the Mazeno Pass pluton (5400 m), a notably undeformed, tourmaline and biotite absent, fine-grained muscovite granite yields discordant zircon ages having an upper intercept of 1860 Ma, typical for the Precambrian protolith of the NPHM, and a young cluster of concordant ages at ~1.4 Ma; monazite from the same sample yields a Th-Pb age of ~1.4 Ma as well. A staurolite-kyanite-garnet schist sampled from near the village of Tarshing yields discordant U-Pb zircon ages which fall along a chord extending from ~1860 Ma to < 5 Ma.

In the northwestern portion of the NPHM ("Haramosh area"), the Jutial granite is predominantly a two-mica, tourmaline granite, essentially undeformed. Two samples yielded concordant U-Pb zircon ages of 10±1 Ma. A second igneous phase was also examined; this yielded a Th-Pb monazite age of 5.2±0.3 Ma. Previously reported biotite and muscovite Ar/Ar cooling ages from the Jutial granite are ~5-6 Ma (George et al., 1995).

Along the southeastern margin of the NPHM, both biotite schist and the eastern edges of a ~NE-SW trending, several-km-thick, extensive belt of S-C fabric porphyroclastic granitic augen gneiss (Rupal Shear Zone) give total-fusion Ar/Ar ages of > 15 Ma. These differ sharply from the young ages west and north of the Rupal shear zone (< 3 Ma) and indicate a marked contrast in recent exhumation history. A suite of total-fusion Ar/Ar biotite ages from the southwestern NPHM, 15-20 km west of Mazeno Pass, define an even larger age contrast, with ages of between 20 and 30 Ma occurring in these Indian plate cover metapelites. Between here and Mazeno/Toshe Gali, a steep ~NNE striking normal fault can be traced to either the Raikot/Liachar Thrust (locally the western margin of NPHM) or to the Tato shear in the Raikot Valley.

We conclude that structures substantially inboard of the W & E margins have accommodated block uplift of Nanga Parbat. In addition to providing precise ages to identify thermal events and associated thermal and mechanical boundaries, our new data have modified and refined the data array illustrated in Winslow et al. (1996). This now shows that within NPHM there has been differential exhumation and magmatism from north to south (younger in south) reaching sufficiently large and localized displacements of mass to involve major intra-massif shear zones.

G42D-6 1635h

**Himalayan Tectonics With A Grain of Salt: A View From the Left-Hand Edge**

PO Koons (Dept. of Geology, University of Otago, PO Box 56, Dunedin, New Zealand; ph. 00643 479-7509; e-mail: Peter.Koons@stonebow.otago.ac.nz); PK Zeitler (EES Dept., 31 Williams Drive, Lehigh University, Bethlehem, PA 18015-3188, USA; ph. 610-758-3671; e-mail: pks0@lehigh.edu)

The enduring image of the Himalaya and the Tibetan Plateau forming in response to a symmetrical India punching north into Asia ignores the structural, topographic and geological asymmetry of the orogen. The eastern margin of the Himalaya near Namche Barwa exhibits the characteristics of an indenter corner where convergence becomes discontinuous. Vorticity is high adjacent to the corner and the great topographic relief is dominated by steep strike-slip faulted valleys. On the western margin, the Indian plate massif of the Nanga Parbat-Haramosh (NPHM) protrudes as far north as the eastern syntaxis and, as in the east, the major drainage exits the Plateau/Karakoram through this protrusion. However, evidence for major sinistral strike-slip displacements associated with significant vorticity along this margin is absent, the topographic pattern is more complex, and there is no obvious discontinuity in the convergence at this western margin.

The timing of metamorphism and exhumation along the western margin is rather different from that observed elsewhere in the Himalaya, with widespread evidence for early collision and peak metamorphic conditions hav-

ing taken achieved by 45 to 60 Ma. Whereas most regions of the Pakistan Himalaya are marked by broad monotonic trends in postmetamorphic cooling history, all at modest rates, the region centered on the Nanga Parbat massif has experienced metamorphism and anatexis over the past 3.3 Ma, followed by extremely rapid cooling associated with exhumation rates of about 5 km/m.y. Complementing the record preserved in the hinterland, sediments of the Siwalik molasse record some 18 Ma of detailed information about tectonic events in foreland. Of particular significance, these sediments record the emergence of the Salt Range thrust between 5 and 6 Ma, suggesting that broadening of the foreland and reduction of its critical taper took place at about this time.

Three-dimensional numerical modeling of the western margin, constrained by geological and geochronological data, permits linking of deformation in the NPHM and the foreland. The rapid exhumation of the NPHM results from strain focussing through non-linear interaction of thermal, strain and erosional weakening of the thickening Indian crust. This tectonic aneurysm is associated temporally and spatially with reduction of the western lateral restraint as the Himalayan foreland in Pakistan extrudes along weak, basal salt beds. Under these conditions, the western Himalayan margin evolves to resemble the eastern margin, but this superficial resemblance is not due to similar plate bounding geometries.

G42D-7 1650h

**Continental escape, non-uniform slip, and seismic hazards along Xianshuihe Fault, China**

Lanbo Liu (Dept. of Geology & Geophysics, Univ. of Connecticut, Storrs, CT 06269-2045; ph. 860-486-1388; e-mail: lanbo@geol.uconn.edu); Peter Malin (Dept. of Geology, Duke Univ. Durham, NC 27707; ph. 919-681-8889; e-mail: pem@vaino.geo.duke.edu); Weibin Han (seismological Bureau of Sichuan Province, Chengdu, 610041, P. R. China;

The Sichuan-Yunnan block is the largest intraplate unit in the eastern edge of the Tibetan Plateau. This block is translating to southeast at a rate of 8-10 mm/a (Ma, et al, 1989). This motion is considered a prime example of "continent escape", in this case resulting from the north-south compression of Indian-Eurasian collision. The left-lateral strike-slip Xianshuihe fault forms the northeast boundary of the Sichuan-Yunnan block. The accumulated Cenozoic slip along this fault is about 60 km (Burchfiel et al 1995). The Xianshuihe fault has been highly seismically active in modern times, producing some four M7 earthquakes per century (Wen et al 1996). The average Holocene slip rate along its north-west portion is about 15 mm/yr; along its southern portion the slip is about 5-7 mm/yr. (Allan, 1991; Wen et al 1996). Short baseline cross fault surveys at Xialatuo up to 1990 have revealed a total of more than 24 cm strike-postslip after the 1973 Ms=7.9 Luhuo earthquake (Bilham, 1992). Directly south of the creeping Luhuo-Daofu segment, between Daofu and Qianing the Xianshuihe fault is essentially locked (Han et al 1992). The continental dynamics question posed by this nonuniform slip along Xianshuihe fault concerns the rate of stress and strain accumulation along the Daofu-Qianing segment. Numerical modeling using the Discontinuous Deformation Analysis (DDA) suggests an accelerating stress build up on this segment. The build up is caused by the joint effects of block motion and slip heterogeneity along the fault. If correct, the postulated stress build up poses considerable earthquake hazard and risk for this part of China. To address this question, we propose that a continuous GPS and microearthquake study of the Luhuo-Daofu/Daofu Qianing fault segments be mounted. In this presentation we discuss our DDA modeling results and the requirements of the proposed study.

## Reference Style for Abstracts

When referencing a meeting abstract, please use the following format, which indicates that this abstract volume is a supplement to the regular *Eos* issue. This format meets all AGU requirements for a complete reference.

Jackman, C. H., Solar energetic particle effects on stratospheric constituents, *Eos Trans. AGU*, 78(17), Spring Meet. Suppl., S203, 1997.

G42C-2 1345h

## EOP Temporal Signatures in the 77-day CONT96 VLBI Campaign

T A Clark, J M Gipson, C Ma, J R Wyan and N R Vandenberg  
(Laboratory for Terrestrial Physics, Goddard Space Flight Center,  
Greenbelt MD 20771; 301-286-5957; clark@tomcat.gsfc.nasa.gov)

During the period Sep.2 through Nov.15 1996, a special VLBI EOP campaign named CONT96 was conducted by NASA's Space Geodesy Program using a 5-station network extending from Europe to Hawaii. The goals for CONT96 were to achieve daily determinations of UT1 with uncertainties of  $\leq 3 \mu\text{sec}$  (1 $\sigma$ ) and PM/nutation of  $\leq 75 \mu\text{arcsec}$ .

Twenty-four one-day observing sessions spanning the 11-week period were scheduled. Within each week, the 4-element zero-redundancy "Arsac" sequence (1100101) was used. Six such week-long groups were scheduled in a minimum-redundancy sequence spanning the entire 77 days. This approach allowed a complete spectral sampling spanning the entire sub-daily to monthly range with an operational "cost" of only ~30% of a fully continuous program.

Coincident with six of the CONT96 measurement days we observed with an independent 12-station network composed of the entire 10-element Very Long Baseline Array (VLBA) augmented by two European stations. The operational 4 or 5-station NEOS Earth orientation program produced normal weekly EOP determinations during the entire CONT96 period (observing on one of the "zero" days of the Arsac 1100101 sequence).

At the time of this writing, about 80% of the VLBI data have been correlated and all are of excellent quality. Baseline lengths from the CONT96 data show fractional repeatability of  $\sim 0.8 \times 10^{-9}$ . Analysis techniques for extracting temporal EOP signatures from non-uniformly spaced data will be described.

G42C-3 1400h INVITED

## Routine Sub-Daily ERP Determination at the CODE Analysis Center of the IGS

M Rothacher; T Springer; G Beutler (AIUB, Berne, Switzerland, CH-3012; ph. 0041-31-631-8591; e-mail: rothacher@aiub.unibe.ch); R Weber (TU Vienna, Vienna, Austria, A-1040; ph. 0043-158-801-3795; e-mail: rweber@terra.tuwien.ac.at)

The Center for Orbit Determination in Europe (CODE) is one of seven IGS Analysis Centers. It uses the GPS data of the global IGS network to routinely compute orbits, site coordinates, earth rotation parameters (ERPs), and other global products.

Since day 084 (March 24), 1996, a special global 3-day solution is produced every day at CODE to determine sub-daily ERPs, i.e. the x- and y-pole coordinates and LOD. The ERPs are estimated as linear functions within each 2-hour time interval enforcing continuity at the interval boundaries. This means that by now more than one year of routine sub-daily ERP estimates are available. In addition, all the GPS data from January 1, 1995, up to the start of the routine series in March 1996, have been reprocessed (in two phases), thus extending the time interval covered by sub-daily ERP series to a total of about 2.4 years.

In this contribution we will analyse these ERP series and present sub-daily ERP models derived from these series. The GPS-derived models are compared with models obtained from many years of VLBI or SLR data. The orbit model for the GPS satellites was changed more than once during the period considered. Special emphasis is therefore put on the impact of the orbit model differences on the sub-daily ERP series.

G42C-4 1415h INVITED

## Pressure and Gravitational Torques and Exchanges of Atmospheric Angular Momentum

David A. Salstein and Haig Iskenderian (Both at: Atmospheric and Environmental Research, Inc., 840 Memorial Drive, Cambridge, MA 02139; 617-547-6207; e-mail: salstein@aer.com)

Olivier de Viron and Véronique Dehant (Both at: Royal Observatory of Belgium, 3, avenue Circulaire, B-1180 Bruxelles, Belgium; 32-2-3730201; e-mail: deviron@oma.be)

The atmosphere and solid Earth can be viewed as exchanging angular momentum with each other by means of a number of torque mechanisms. Of the tangential and normal forces on the atmosphere's lower interface, the normal forces against the non-uniform topography appear to be most responsible for rapid changes in angular momentum about the Earth's axis. Recent work has shown that the high variability in the mountain torque that arises from zonal pressure gradients along the Earth's orography is derived mostly from only a few mountain ranges and this variability is strongest in the winter seasons of both hemispheres. When compositing events relative to the timing of strong submonthly fluctuations, the general surface pressure patterns near mountain ranges can be discerned; the Rockies, Andes and Himalayas are most responsible for such a fluctuation. The atmosphere and solid Earth also interact through body forces by gravitational attraction. For example, between the diurnal and monthly time scales, the signals of such corresponding gravitational torques on the atmosphere and solid Earth about the axis appear to be an order of magnitude smaller than that of the dominant mountain torques, but nevertheless, this gravitational torque may be needed to reduce the remaining uncertainties in the global angular momentum budget on these time scales.

G42C-5 1430h INVITED

## Modeling Short-period Tidal Variations in Earth Rotation: A Review

R D Ray (STX, NASA/GSFC, Code 926, Greenbelt MD 20771; 301-286-3691; ray@nemo.gsfc.nasa.gov); B F Chao (Space Geodesy Branch, NASA/GSFC, Greenbelt); G D Egbert (Oregon State University, Corvallis, OR).

We review the history, current status, and future prospects of modeling short-period (diurnal and subdiurnal) tidal variations in the earth's rotation. Beginning with early work by Yoder, Baader, Brosche and their colleagues, and continuing through to Seiler's and our own work, progress in modeling accuracy has roughly matched progress in measurement accuracy, with present uncertainties in both around 1 or 2  $\mu\text{s}$  for  $M_2$  UT1 variations. (Modeling uncertainties for diurnal tides are double that.) For modeling earth rotation, Schwiderski's ocean-tide model is presently as accurate as Topex/Poseidon-based models, an initially surprising fact given the known elevation errors in the former; the reason rests with the dominant role of tidal currents in the angular momentum integrals—T/P is only slowly improving our knowledge of currents. Examining the role of deep-water and shallow-water elevations and currents, we find that T/P has accurately constrained deep-water elevations and that shallow-water currents are of little significance owing to their very small transports. Progress depends on improving deep-water currents and shallow-water elevations. Present work in assimilation methods are improving the former; the latter will require detailed local hydrodynamic modeling for many shallow seas and bays where present knowledge is inadequate—a slow and difficult task. Assimilation models that exploit generalized inverse methods will also help establish more rigorous error bounds, accounting both for data errors and for errors induced by faulty dynamical assumptions used to infer currents. We also address the role of atmospheric tides, which are required for modeling  $S_1$  and  $S_2$  motions.

G42C-6 1445h INVITED

## Oceanic Forcing of Length-of-Day Variations Detected by a General Circulation Model

Steven L. Marcus (Jet Propulsion Laboratory, 4800 Oak Grove Dr., Pasadena, CA, 91109 U.S.A.; ph. 818-354-3477; e-mail: SLM@LOGOS.JPL.NASA.GOV); Jean O. Dickey (Jet Propulsion Laboratory, 4800 Oak Grove Dr., Pasadena, CA, 91109 U.S.A.; ph. 818-354-3235; e-mail: JOD@LOGOS.JPL.NASA.GOV); Yi Chao (Jet Propulsion Laboratory, 4800 Oak Grove Dr., Pasadena, CA, 91109 U.S.A.; ph. 818-354-8168; e-mail: YC@COX.JPL.NASA.GOV)

Non-tidal changes in the length-of-day (LOD) on time scales of a few years or less are largely caused by concomitant fluctuations in atmospheric angular momentum (AAM). In recent years, increasingly accurate determinations of Earth orientation by space geodetic methods, as well as the growing capability to model the global atmosphere, have led to the detection of residuals which can be attributed to oceanic effects. In this study, we use an oceanic GCM forced by NCEP surface winds to identify seasonal as well as sub-seasonal contributions to the Earth's axial angular momentum budget caused by variations in the motion and mass fields of the world ocean.

The ocean model is based on the 3-dimensional primitive equations, and employs realistic bottom topography. Because the model does not conserve mass, corrections were applied to the planetary angular momentum term, using both the average PAM per unit mass, as well as the PAM contained in a uniform surface layer. Both methods give similar results, and show significant correlations between the computed oceanic angular momentum and the residual between LOD and AAM forcing over a three-year observational period (1992-1994). Oceanic contributions to the annual and semi-annual components of the angular momentum budget are presented, along with coherence at intraseasonal time scales.

## G42D CC: 325 Thurs 1520h

### Edge Mechanics and Internal Deformation of the Tibetan Plateau (joint with S, T)

Presiding: R Bendick, Univ of Colorado;  
R Bilham, Univ of Colorado

G42D-1 1520h INVITED

## Morphotectonic Evolution of the Tibetan Plateau

E J Fielding (Jet Propulsion Lab\*, CalTech, Pasadena, CA, 91109 USA; ph. 1-818-393-3614; e-mail: Eric.Fielding@jpl.nasa.gov)

The surface of Tibet records the integrated effects of tectonic and erosional processes over at least 20 million years, but it is most sensitive to more recent effects that have tended to erase evidence of earlier processes. The maximum elevation and consequent change to an extensional regime of the Tibetan Plateau are likely to have resulted from some type of lithospheric thinning process. Extension and volcanism, indicate that it probably happened by 8 Ma. The apparently sudden development of major structures in southernmost Tibet and the Himalaya at ~25 Ma record a change in the deformation regime that

suggests that the lithospheric thinning may have begun then. One may speculate that the crust of the interior of Tibet between 25 Ma and 8 Ma remained about the same thickness, since it appears that deformation was concentrated in southern Tibet and the Himalaya between ~25 and ~8 Ma, while the mantle lithosphere was thinned dramatically sometime during the Miocene. If this scenario is correct, then this amount of thinning would result in about 3.2 km of uplift of the surface of Tibet between 25 and 8 Ma without a change in crustal thickness.

At moderate-to-long wavelengths from 10 km to hundreds of km, central Tibet is extremely flat. This lack of long-wavelength relief may be caused by flow in the lower crust due to the extreme thickness of and heat production within the Tibetan crust or other processes that result in a low effective viscosity of the lithosphere. Flexural modeling of the rift flank uplift on some of the graben in Tibet suggests a very thin effective elastic plate thickness (< 10 km) that would be consistent with a low viscosity zone in the Tibetan crust. The low rates of fluvial cut-and-fill processes for central Tibet cannot erase tectonic relief at moderate wavelengths, so either there has been little significant deformation of the upper crust in the late Cenozoic or some other process, such as viscous flow in the lower crust, has removed relief at these wavelengths.

\* This work was carried out by the Jet Propulsion Laboratory, CalTech, under contract with NASA.

G42D-2 1535h INVITED

## Strain partitioning as applied to Southern Tibet

Robert McCaffrey (Dept. of Earth and Environmental Sciences, Rensselaer Polytechnic Institute, Troy NY 12180; ph. 518 2768521; e-mail: robmcc@geo.rpi.edu)

Strain partitioning occurs to some degree at most of the world's subduction zones. It is most commonly revealed by interplate thrust earthquake slip vectors that are more perpendicular to the plate margin than is the plate convergence vector. Kinematically, the slip vector deflections indicate that there is some permanent deformation of the overriding forearc and the most common type is arc-parallel translation and extension. The upper-plate extension is expected to occur over the curved, dipping plate boundary and the translation occurs by strike-slip faulting above or landward of the downdip edge of plate coupling. At some subduction zones, earthquake slip vectors remain perpendicular to the trench through large changes in its orientation, which probably means that the upper plate can withstand very little lateral shear stress elastically. Recent GPS results from Sumatra (Prawirodirdjo et al., Science, submitted) show complete partitioning of the strain, including arc-parallel extension, in accordance with inferences made from slip vectors. Similarly, slip vectors for thrust earthquakes at the Himalayan deformation front are nearly perpendicular to it throughout its length. GPS results of Bilham et al. (Nature, in press) for Nepal reveal strain partitioning and block-like behavior of S Tibet, similar to Sumatra and the Aleutians. Considering that India subducts a distance of at least 100 km beneath S Tibet, we can make the analogy between the Himalayan front and an oblique subduction zone. The radial slip vectors and principal strain directions in Nepal, extension is S Tibet on N-trending normal faults, and right-lateral faulting along the Karakorum - Jiali fault zone are reminiscent of patterns of strain partitioning in subduction zones. If so, this implies that some part of Indian lithosphere extends well under S Tibet, possibly as far as the Karakorum - Jiali fault zone.

G42D-3 1550h

## The Himalaya from its Pole of Extrusion: Morphology and Collisional Kinematics

Rebecca Bendick; Roger Bilham (CIRES, University of Colorado, Boulder, CO 80303-0216 USA; ph. (303)492-0382; e-mail: becky@creep.colorado.edu)

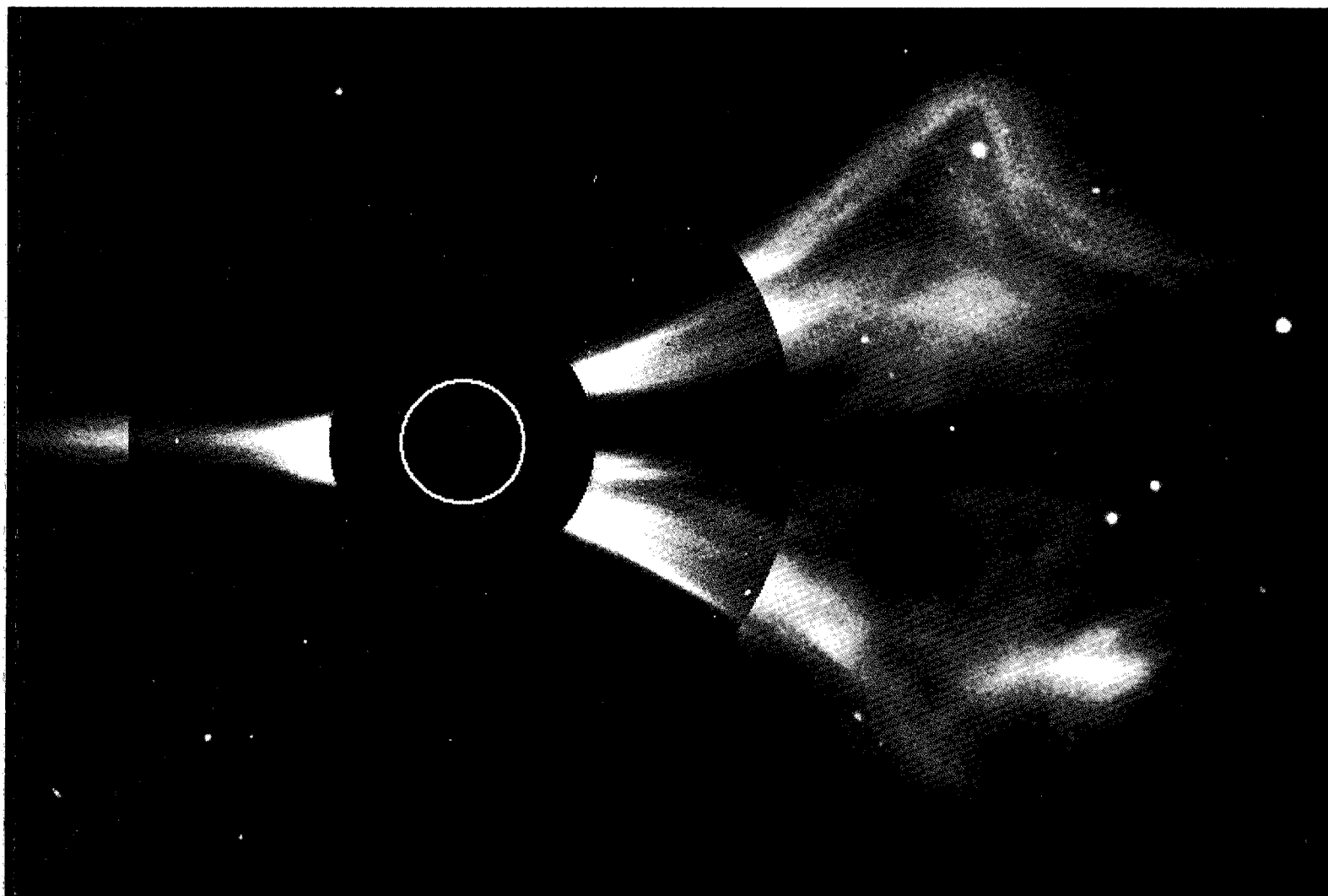
The region of active uplift at the Himalayan front defined by seismicity and knickpoints in river profiles corresponds to a small circle centered in Siberia. The pole of this circle can be considered the pole of extrusion of the southern Tibetan Plateau. In this reference frame it is evident that the radius of the Himalaya,  $R$ , is given by  $R = v/\epsilon$  where  $v$  is the velocity of arc-normal collision between Tibet and India, and  $\epsilon$  is the along-arc strain in southern Tibet. Since  $R=1696$  km (Seeber and Gornitz, 1983), and  $v = 20.5 \pm 2$  mm/a from GPS studies, we calculate that  $\epsilon = 12$  nanostrain/year.

By projecting the Himalaya on a Mercator projection centered on this pole of extrusion, structural characteristics of the collision process are significantly enhanced and can be subjected to quantitative interpretation. Arc-parallel buckles with an approximate wavelength of 100 km show that compressional forces are everywhere perpendicular to the arc. Extensional features with an approximate spatial separation of 50 km are perpendicular to the arc and therefore radiate from the pole.

In particular, we find that the position of the peak in mean Himalayan along-arc relief deviates by less than 15 km from this small circle along more than 1000 km of the arc. The position of this relief peak in Nepal has been hypothesized to link to the tip of a dislocation beneath Tibet such that the Indian plate is locked to its south, and sliding aseismically beneath Tibet to its north. Hence the mapped position of the peak in mean relief may represent the tip of this dislocation along the entire Himalaya. The deviation of the peak from the calculated small circle

# 1997 SPRING MEETING

American Geophysical Union



Published as a supplement to *Eos*, April 29, 1997

